Local molecular order in the biaxial smectic mesophase of HpAB: A proton-^{14}N cross relaxation study

E. Anoardo and D. J. Pusiol
Facultad de Matemática, Astronomía y Física, Universidad Nacional de Córdoba, Ciudad Universitaria, 5000 Córdoba, Argentina
(Received 11 September 1996)

Proton spin-lattice relaxation dispersion has been carefully measured at the Larmor frequency range from 3 kHz to 4 MHz in the smectic-*C* mesophase of 4-4′-bis-heptyloxy-azoxy-benzene (HpAB). Measurements were carried out by means of the fast field cycling NMR technique. The stability and precision of the low relaxation magnetic field has been tested by scanning the proton resonance with a second irradiation frequency. Three chemically inequivalent nitrogen nuclei have been detected, denoting the existence of two nonequivalent molecules. We conclude that a bimolecular structure can be associated with the elemental liquid crystalline unit. [S1063-651X(97)15505-2]

PACS number(s): 61.30.Eb, 42.70.Df, 64.70.Md, 61.30.Gd

I. INTRODUCTION

Cross relaxation nuclear quadrupole resonance (NQR) spectrum in liquid crystals (LC's) has been established to be a powerful technique for studying local molecular ordering, i.e., local order parameters [1,2]. The main advantage is due to the easy identification of the NQR nuclei spectrum in comparison with the always complex proton NMR spectra. Conventional NQR experiments in liquid crystalline mesophases have, up to now, been unsuccessful, mainly due to two facts: (i) the relative low abundance of quadrupole nuclei even in the simplest LC molecules, and (ii) the strong averaging of electric field gradients (EFG's) at the quadrupole sites. However, NQR has been indirectly measured via both crossover relaxation in the laboratory frame at a fixed relaxation period [1], and proton Zeeman-quadrupole cross relaxation techniques [3,4]. We used the latter because it allows us to obtain information about the spectral densities.

Quadrupole dips (QD's) appear in the proton spin-lattice relaxation dispersion $[T_1(\nu)]$ when ^{1}H and quadrupole nuclei relax through level crossing [5]. By scanning the external magnetic field, ^{1}H nuclei will undergo a second relaxation process just when both level systems match. This effect produces a dip in the $T_1(\nu)$ dispersion curve. In the case of ^{14}N nuclei sensing an EFG with a nonzero asymmetry parameter, three QD's are generally expected [6]: one at low frequency and a doublet at higher frequency.

A few years ago ^{14}N QD's were measured in several well-known smectogen and nematogen liquid crystals [para-azoxyanisole (PAA), cyano-biphenyls (CB), and oxy-cyano-biphenyls (OCB) series] [3,7,8]. Due to the relative short spin-lattice relaxation time of protons in those samples, the experiments were carried out using the fast field cycling NMR technique [9,10]. QD's presenting smaller widths were also measured in ethoxybenzidenbutylanilin (EBBA) by Dvinskikh and Molchanov [11]. In order to verify previous data, new measurements were performed at Stuttgart using a new field cycling spectrometer [12]. The results do not keep agreement in the QD spectral parameters, i.e., between their widths, frequency positions, and peak shapes. Although there is reasonable agreement between values of the $T_1(\nu)$ background. Table I presents the results obtained by different authors.

In order to check the existence of QD's as a physical phenomena, and not as an undesirable consequence of the complicated fast field cycling NMR technique, we recently tried to find QD's by a conventional NMR experiment [4]. The 4-chlorophenyl 4-undecyloxybenzoate is a smectogen compound having a chlorine atom bounded to the benzene ring. The quadrupole moment of the ^{35}Cl nuclei is approximately an order of magnitude higher than the ^{14}N one. Therefore, dip frequencies have been found in the range 15–30 MHz.

In a recently published work [13], we have studied the smectic-*C* phase (Sm-*C*) of 4,4′-heptyloxyazoxybenzene (HpAB), with special attention in the experimental aspects which could distort the shape and frequency of QD's:

(1) *Stability and precision of the Zeeman field during the level crossing period*. Temporal variations of relaxation field B_r are expected to be observed as an extra broadening in the QD shapes.

(2) *Temperature gradient along the sample*. As has been previously shown [8], κ and η vary with temperature; gradients might then distort both width and central frequency.

(3) *Purity of the sample*. Impurity molecules could contribute to an extra dispersion of the electric field gradients at the ^{14}N sites, producing an extra broadening of the NQR line.

The experimental conditions of our experiment allow the detection of eight high frequency QD's, instead of the previously reported four [3]. The widths are similar to those measured by Dvinskikh and by Zollino. The number of QD's we

TABLE I. HpAB at $T=82$ °C quadrupole dips, measured by different authors.

Author	ν_0	ν_-	ν_+	Width (ν_-)	Compound	T °C
Pusiol	13	250	2300	150	HpAB	82
	23	510	2600			
Zollino	18	439		10	HpAB	82
		695				
Dvinskikh	16.6	649	668	8	EBBA	40
Zollino	8.4	641	654	2	EBBA	40

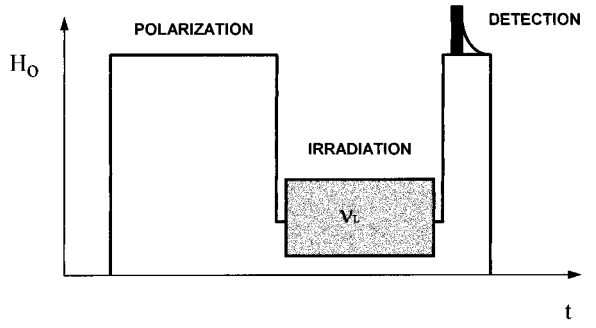

FIG. 1. Magnetic field and rf pulse sequence used to check the relaxation magnetic field stability. The magnetization of a sample of water is destroyed during the relaxation period by irradiating the protons at the low field Larmor frequency.

report in this work indicates that there are two chemically nonequivalent molecules in the Sm-*C* of HpAB. The phenomenon is explained assuming that the mesophase is composed of bimolecular units. In the present work, details of the experiment, and data for the low frequency dips are given.

II. EXPERIMENT

The above last three experimental requirements were achieved by a careful measurement of temperature gradients along the sample volume, by proper data processing and by repeated recrystallization of the sample as a purifying method.

We tested B_r by means of a double resonance experiment in a sample of water where no QD takes place. During the relaxation period, the water is irradiated with a second rf pulse of frequency ν_r (Fig. 1). Absorption of the second frequency is produced just as the relation $\gamma B_r = \nu_r$ is met. The quantity $\gamma \Delta \nu_r$, which is extracted from the rf absorption as ν_r is conveniently scanned, gives us a measure of the time dispersion of B_r.

The fast field cycling NMR spectrometer is based on a specially designed air cored 0.5-T low resistance electromagnet [14]. The electronics of the magnetic field switch and control was entirely homemade in our Laboratory [15]. The 17-MHz high field NMR transmitter-receiver is a Matec Mod. 6600. The free induction decay signal is digitized by a computer-controlled Biomation Mod. 805 wave form digital recorder. The second frequency source is a Schlumberger Mod. 4431 synthesizer which is pulsed by a home-made pulse programmer.

The same rf coil is used for irradiation at both ν_L and ν_r. A reed relay bank connects that coil with the respective high and low frequency resonant circuits.

A personal computer controls the main spectrometer functions. A second computer is used to run the spectrometer security system.

Additional pulsed coils are used for shimming the detection magnetic field. The earth magnetic field is compensated for by an external pair of dc-driven Helmholtz coils.

In the frequency range of interest we have a dispersion in B_r of approximately 0.5% (for $\nu_r = 400$ kHz) and 0.1% (for $\nu_r = 2$ MHz), respectively. Very fine adjustments of the B_r electronic control were necessary before reaching the final performance.

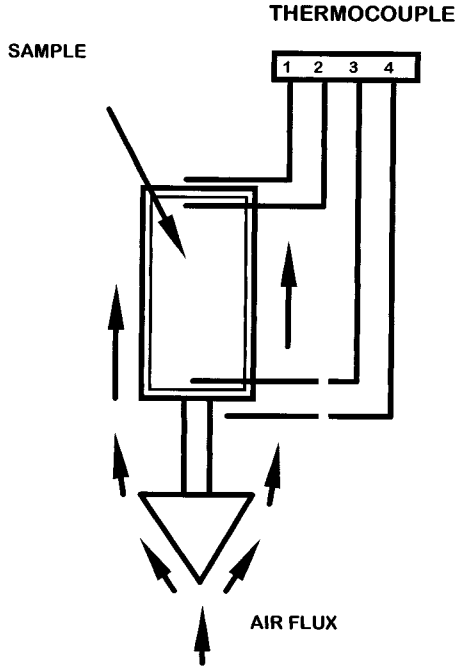

FIG. 2. Experimental setup used to check temperature gradients along the sample. Four *K*-type calibrated thermocouples have been located at the top and bottom of the sample, and inside and outside the sample. A conic device was used to avoid overheating at the bottom of the sample (see text).

Four *K*-type calibrated thermocouples have been located at the top and the bottom and inside and outside of our liquid crystalline sample (Fig. 2). A conic device was installed in the rf coil, so that the flux of hot air can circulate around it without overheating the bottom of the sample. This point turns out to be very important. No gradients higher than 0.5 °C/cm have been detected while the sample was heated up to 150 °C.

Data reduction was carried out by both homemade and commercial software. Commercial E. Merck HpAB was recrystallized several times from a solution with pure proanalysis ethanol, until a yellow and crystalline solid was obtained. After each recrystallization, fusion and clearing points were checked. Only after no changes in both melting and clearing points were detectable was the purification process stopped.

The thermal treatment of the sample was the same as in previous experiments. It was heated to the isotropic phase and maintained at $T = 130$ °C for about 10 min (a narrow NMR line was used to check the liquid isotropic state). In the following step, the sample was cooled to the Sm-*C* mesophase after crossing the nematic phase at $T = 82 \pm 0.5$ °C. At this stage, the NMR signal was again used to check the successive phase transitions. Before starting the $T_1(\nu_L)$ measurements, the sample was left at the working temperature for about 1 h. During the thermal cycle the sample was located in the probe head, with the spectrometer magnetic field set at 100 mT. The purity of the sample was always checked after measurements, and data taken on decomposed samples were discarded. Several experiments at different cooling rates (lasting for 20, 90, and 180 min), taken from the isotropic phase, were carried out in the high frequency range

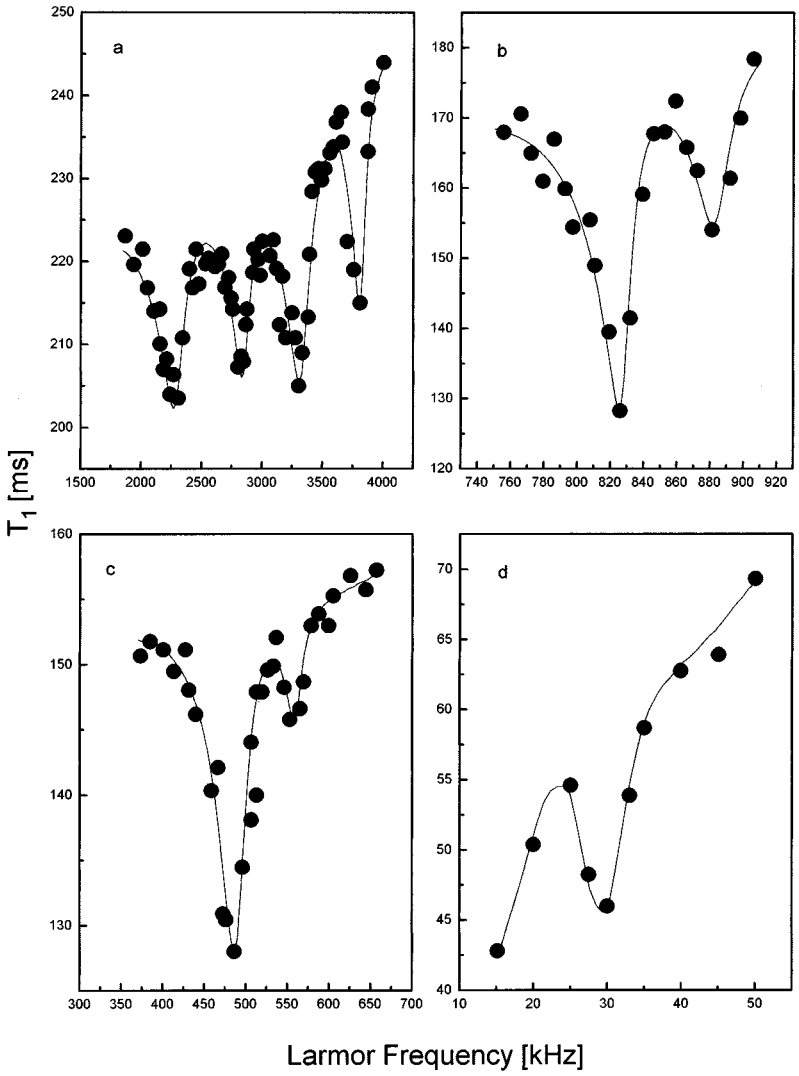

FIG. 3. Experimental results of $T_1(\nu_L)$ of Sm-C HpAB at $T=82\,^{\circ}$C. Nine $T_1(\nu_L)$ quadrupole dips have been found. Two chemically nonequivalent HpAB molecules are present in the Smectic-C liquid crystalline phase.

QD's. Within experimental errors the $T_1(\nu_L)$ curves were found to be almost independent of the cooling rate.

III. RESULTS AND DATA ANALYSIS

Nine QD's can be distinguished from the experimental $T_1(\nu)$ dispersion plotted in Fig. 3. $T_1(\nu)$ shows a dip centered at 30 kHz. Also, a doublet at Larmor frequencies close to 450 kHz can be distinguished. In addition, a second pair of QD's was found in the neighborhood of 700 kHz. In the MHz regime other two doublets are resolved. The observed widths are approximately 20 kHz, in agreement with Zollino's data [12].

The total Hamiltonian of the ^{14}N nuclei can be expressed as $H=H_Q+H_M$ with [10]:

$$H_Q=\sum_{m=-2}^{2} Q_2^m V_2^{-m}, \tag{1}$$

where

$$Q_2^0=\frac{eQ}{2}[3I_z^2-I(I+1)], \quad V_2^0=(1/2)eq,$$

$$Q_2^{\pm 1}=\frac{eQ\sqrt{6}}{4}[I_zI_{\pm}+I_{\pm}I_z], \quad V_2^{\pm 1}=0,$$

$$Q_2^{\pm 2}=\frac{eQ\sqrt{6}}{8}I_{\pm}^2, \quad V_2^{\pm 2}=(1/2\sqrt{6})\,\eta eq.$$

$\kappa=(e^2qQ)/h$ is the quadrupolar coupling constant and η the asymmetry parameter of the electric charge distribution around the nucleus. The irreducible quadrupolar tensor components Q_2^m are defined in the laboratory (x_L,y_L,z_L) frame with the z_L axis parallel to the direction of the external magnetic field H_0. The components of the electric field gradient tensor V_2^{-m} are defined in the principal axis frame. In the limit of weak Zeeman field, we had to consider the possibility that H_M and off diagonal elements of H_Q are comparable. In this case, the high frequency resonances for $I=1$ spin are

$$\nu_+=\frac{1}{2\pi\hbar}[3A+\sqrt{(\hbar\Omega\,\cos\Theta)^2+(A\eta)^2}], \tag{2}$$

$$\nu_-=\frac{1}{2\pi\hbar}[3A-\sqrt{(\hbar\Omega\,\cos\Theta)^2+(A\eta)^2}],$$

$A=(e^2qQ)/4=(\pi\hbar\kappa)/2, \Omega=\gamma_N H_0$, where γ_N is the magnetogiric ratio of ^{14}N nuclei, and Θ is the angle between the z principal axis and laboratory frame z axis.

These expressions are valid for a monocrystalline sample. As liquid crystals molecules are oriented by the external field due to their magnetic anisotropy [16], we can think the mesophase as a monocrystalline sample rather than a powder one. In a powdered sample the values of Θ are randomly distributed, but in the smectic-C under the application of a magnetic field, molecules can be aligned along the field [17] (we can think of an averaged Θ over molecular ordering distributions). In the case of magnetic field cycling, the system reaches an equilibrium orientational configuration. In order to begin the experiment with molecules oriented with the field, the sample was heated to the clearing point immersed in a constant field of about 100 mT, and then cooled to the smectic. This is an important procedure to guarantee a good orientational order in the external field before starting measurements. For example, important differences in the ^{2}H spectra taken in the smectics-E were observed between recorded signals before and after the mentioned heating-cooling process [18]. Fields up to 1 T were reported to be necessary to orient molecules in smectics-C [19]. However, we have found that few tens of mT are enough to induce molecular order in HpAB. Once the smectic director is oriented in the field, we can suppose the magnetic field timing is faster than the molecular response times. This last statement will be valid depending upon the viscosity coefficients of the compound in the smectic-C [20]. However, in this mesophase, the polar viscosity is of the same order as that of nematic viscosity [21]. Additionally, polar rotational reorientations are expected to be slower than magnetic field variations (see for instance reference [22] for the case of nematics).

At the limit of small $\Theta, A\eta$, and $\hbar\Omega\cos\Theta$ can be comparable. Taking into account the fact that the occurrence of ν_+ and ν_- of each nonequivalent nitrogen is at different Zeeman external fields, we consider an Ω_+ and Ω_- for each line of the doublet:

$$(\nu_+-\nu_-)=\frac{1}{2\pi\hbar}[\sqrt{(\hbar\Omega_+\cos\Theta)^2+(A\eta)^2} + \sqrt{(\hbar\Omega_-\cos\Theta)^2+(A\eta)^2}], \tag{3}$$

from which, approximately,

$$(\nu_+-\nu_-)^2\approx\frac{1}{(2\pi)^2}\left[\Delta^2\cos^2\Theta+\left(\frac{2A\eta}{\hbar}\right)^2\right] \tag{4}$$

where $\Delta^2=\Omega_+^2+\Omega_-^2+2\Omega_m^2$ and $\Omega_m=(\Omega_++\Omega_-)/2$. From Eq. (4), and from the fact that $A\eta=\pi\hbar\nu_0$, where ν_0 is the low frequency resonance of $I=1$ NQR (not affected by the Zeeman term), we have

$$\cos\Theta=\pm\frac{2\pi}{A}\sqrt{(\nu_+-\nu_-)^2-\nu_0^2}. \tag{5}$$

Finally, the values of the quadrupolar constant and the asymmetry parameter can be calculated from $\kappa=\frac{2}{3}(\nu_++\nu_-)$ and $\eta=(2\nu_0)/\kappa$.

TABLE II. NQR parameters of the detected dips calculated from the analysis described in the text.

	N_1	N_2	$N_{3,4}$
ν_+ (kHz)	2840	3800	880
ν_- (kHz)	2260	3300	825
ν_0 (kHz)	560	485	30
Θ (deg)	65.9	76.3	68
κ (kHz)	3400	4733.3	1136.7
η	0.33	0.2	0.05

Table II summarizes dip frequency assignations to the three resolved (four nonequivalent) ^{14}N and their calculated values of Θ, κ, and η. The measured ν_0 value of nitrogen 3 was about 30 kHz, in close coincidence with previous data [11,13]. As can be observed in Fig. 3, the dips of 880 and 825 kHz have double the intensity of the others, indicating that two nonresolved nitrogens can be associated with them.

These results suggest that bimolecular groups are present in the smectic HpAB. The same order was previously found in similar liquid crystalline compounds in the solid [23]. In this reference, it can be clearly observed that the ν_0 line of PAA and HOAB is also split into three dips. Moreover, the solid effect double resonance spectra of ν_0 shows a central line with double the intensity of the other two, corresponding to an evident nonresolved pair of nitrogens of the same bimolecular unit cell.

Transforming the EFG tensor from the principal system to the bimolecular frame with the z axis pointing along the longitudinal symmetry axis, and from that frame to the laboratory, η can be expressed in terms of the Euler angles of the rotations [24]. Taking the Euler angles of the first rotation as (α,β,γ), and that corresponding to the second one as (ϕ,θ,ψ), η can be expressed

$$\begin{aligned}\eta=&\tfrac{3}{2}\{\sin^2\alpha\,\cos2\beta[\langle\cos2\phi(1+\cos^2\theta)\cos2\psi\rangle\\ &-2\langle\sin2\phi\,\cos\theta\,\sin2\psi\rangle]\\ &-2\,\sin2\alpha\,\sin\beta[\langle\cos2\phi\,\sin\theta\,\cos\theta\,\sin\psi\rangle\\ &+\langle\sin2\phi\,\sin\theta\,\cos\psi\rangle]+\langle\sin^2\theta\,\cos2\phi\rangle(3\cos^2\alpha-1)\}\\ &\times\{\langle\tfrac{3}{2}\cos^2\theta-\tfrac{1}{2}\rangle(3\cos^2\alpha-1)\}^{-1}.\end{aligned}$$

If the bimolecular group rotates about the longitudinal axis in a nearly unhindered fashion, but fast compared with the experimental time scale ($\dot{\psi}\gg\omega_Q$), all values of ψ have the same probability. As a consequence, the previous expression simplifies to

$$\eta=\frac{3\langle\sin^2\theta\,\cos2\phi\rangle}{3\cos^2\theta-1}. \tag{6}$$

In this case, η becomes independent of the positions of different nitrogens in the group (the final expression in this limit does not depend on the first rotation). According to this limit, η should be the same for all nitrogens. As is clear from Table II, this is not the present case, and it can be concluded that there exists a rotational freeze-out due to the biaxial character of the Sm-C topology. As shown in Table II, the

unresolved nitrogens have a smaller η, and therefore, these can be associated with sites not bounded to the oxygen of each molecule. The other nitrogens have similar asymmetry parameters, and correspond to the oxygen bonded sites.

The PAA molecule, which has the same molecular core as HpAB, has an angle of about 55° between the N═N bond and the longest molecular axis. In fact, the measured angle is not this one, nor is the tilt of the mesophase. So there is no reason to suppose the N═N bond direction to be that of the EFG. We are studying this point by means of quantum semiempirical molecular electrostatic maps.

$T_1(\nu)$ dip shapes could be explained by the semiempirical model we described in a previous work [4]. The model is based on an idea reported by Blinc to explain NMR and NQR line shapes of incommensurate systems [25]. The model was later extended to NQR line shapes of a bidimensional incommensurate molecular system [26], a molecular glassy alloy [27], and a liquid crystal [4], and for glassy and crystalline coexisting structures in powder samples of As_2O_3 [28]. The statistical distribution of electric field gradients at the ^{14}N sites $[f(u)]$ in the liquid crystal is expanded in series of an order parameter representing the field of mean displacement of such nuclei with respect to the perfect square rigid lattice (u). The density of the spectral NQR line $\rho(\nu_Q)$ is linearly related to $f(u)$ [6]. The shape of QD's $F(\nu_L)$ is therefore deduced in some favorable cases by combining $\rho(\nu_Q)$ with the level-crossing conditions [29]. The final expression of $F(\nu_L)$ for dip shape fits are

$$F(\nu_L)=F_+(\nu_L)+F_-(\nu_L), \tag{7}$$

where

$$F_\pm(\nu_L)=aa_2\int_\infty^0 \frac{\exp\left[-\dfrac{(\chi\pm\xi)^2}{2\sigma^2}\right]}{1+b[\nu_L-\nu_{L_o}-a_2(\xi^2-\chi^2)]^2}d\xi, \tag{8}$$

$$\xi=\left(\chi^2+\frac{2}{a_2}(\nu_L-\nu_{L_o})\right)^{1/2}, \tag{9}$$

$$\chi=\frac{a_1}{a_2}, \tag{10}$$

where ν_{L_o} is the frequency corresponding to the maximum of the ^{14}N NQR line. The solid lines in Fig. 3 represent the computer simulation of the QD's, following Eq. (8). It shows a reasonable agreement with our experiment. The fitting parameters are summarized in Table III.

It can be noted that the model was used to fit data without defining the explicit form of the distortion field u. Physical information about the fitting parameters is precisely contained in this function $u=u(\zeta)$, where ζ specifies the distortion sensitive variables. If the form of the distortion field is known, the parameters of the model can be calculated and compared with the corresponding fitting values. From this comparison, it is possible to speculate fine details of the local molecular order. This work is in progress and all details will be published soon.

TABLE III. Parameters used to simulate the shape of the nine QD's for the smectic phase of HpAB at $T=82$ °C. Brackets signify powers of ten.

$f_{\rm dip}$ (kHz)	a	b (kHz^{-2})	χ	a_2 (kHz)	σ	ν_0 (kHz)
30	0.6	0.2	10	−1[−3]	3	30.5
485	1.1[−3]	6.5[−3]	10	−1.7[−2]	40	490
560	6.5[−4]	1.3[−2]	10	−7[−3]	40	561
825	2[−3]	3[−2]	10	−2[−2]	40	827
880	1.1[−3]	1.1[−2]	10	−1.3[−2]	30	884
2260	3.8[−4]	1.6[−4]	10	−3[−3]	250	2300
2840	4.6[−4]	2.7[−4]	10	−2.3[−3]	250	2858
3300	4.6[−4]	1.7[−4]	10	3[−3]	250	3340
3800	6.5[−4]	6[−4]	10	−2[−3]	250	3825

IV. CONCLUSIONS

Our measurement coincides very closely (in both width and shape) with that of Zollino, but he did not detect the second peak in the pairs [12]. The earliest experimental results [3], using an old fast field cycling spectrometer [30], showed broadened QD's (about 150 kHz). Probably, in that old spectrometer the instabilities of the relaxation field were not successfully controlled.

The nine QD's we found in HpAB indicate at least three chemically nonequivalent ^{14}N nuclei in the Sm-C liquid crystalline phase of HpAB. Therefore, two molecules are nonequivalently arranged in the smectic layers, like pairs. In our knowledge there are no previous NQR spectrum studies of HpAB in the solid state. However, NQR studies carried out on several liquid crystals in the solid state have been reported. Both 4,4′-azoxyanizol, 4,4′-anisalazine, and diheptyloxyazoxybenzene show two nonequivalent molecules in the crystalline unit cell [23]. Comparing the similar molecular geometry of both HpAB and PAA, it could be inferred that nine NQR resonances should be detected in the solid phase of HpAB. Therefore, it should be reasonable to conclude that the bimolecular structure, assumed existent in the solid state, is still preserved in the mesophase.

The three chemically nonequivalent nitrogen sites can also be explained by assuming the sample composed by two—or even more—coexisting mesophases at $T=82$ °C. We may assume that N_1 and N_2 could correspond to a monotropic ordered mesophase (note that the values of κ and η listed in Table II are closely related to that typical of solids [23]), while N_3 and N_4 (having much smaller values of κ and η) may be assigned to a rather fluid Sm-C mesophase. Nevertheless, supercooling of a solidlike structure should be discarded for the following reasons:

(1) The above described thermal treatment was applied to the sample: the Sm-C phase was always reached from the isotropic liquid.

(2) The number of QD's is independent of the cooling rate from the isotropic phase.

(3) The high purity of the sample used in the experiments.

(4) The long time (about four days) the sample was kept at the working temperature during experiments ($T=82$ °C).

We can conclude that both the bimolecular local structure of the Sm-C, together with the two molecular unit generally observed in solids [23], implies that the molecule-molecule

pair interactions in the mesophase remain as a property from the solid state, even when the Sm-*C* was reached from the isotropic liquid phase. In other words, the strong interaction between two adjacent molecules is not broken on going from the solid crystalline to the Sm-*C* liquid crystalline state. The softening of the solid interunit forces is therefore the responsible of the fluidity of the HpAB in its Sm-*C* mesophase. Finally, it seems reasonable to us to propose that this liquid crystal is a disordered solid more than an oriented liquid.

ACKNOWLEDGMENTS

The authors thank the National and Provincial Research Councils (CONICET and CONICOR, respectively), as well as the Fundación Antorchas of Argentina for the financial support of the Project. E.A. acknowledges financial support from the National Research Council, CONICET. D.J.P. acknowledges financial support from CONICET.

[1] J. Seliger, R. Osredkar, V. Žagar, and R. Blinc, Phys. Rev. Lett. **38**, 411 (1977).
[2] R. Blinc, J. Dolinsek, M. Luzar, and J. Seliger, Liq. Cryst. **3**, 663 (1988).
[3] D. Pusiol and F. Noack, Liq. Cryst. **5**, 377 (1989).
[4] E. Anoardo, D. Pusiol, and C. Aguilera, Phys. Rev. B **49**, 8600 (1994).
[5] F. Winter and R. Kimmich, Mol. Phys. **45**, 33 (1982).
[6] T. P. Das and E. Hahn, *Nuclear Quadrupole Resonance Spectroscopy*, Solid State Physics Series, Suppl. 1 (Academic Press, New York, 1958).
[7] D. Pusiol and F. Noack (unpublished).
[8] D. Pusiol, R. Humpfer, and F. Noack, Z. Naturforsch. **47a**, 1105 (1992).
[9] F. Noack, Prog. Nucl. Magn. Res. Spectrosc. **18**, 171 (1986).
[10] R. Kimmich, Bull. Magn. Res. **1**, 195 (1980).
[11] S. Dvinskikh and Y. Molchanov, Kimicheskaya Fiz. **10**, 1204 (1991).
[12] P. Zolino, Diplomarbeit, Universität Stuttgart, 1993 (unpublished).
[13] E. Anoardo and D. J. Pusiol, Phys. Rev. Lett. **76** , 3983 (1996).
[14] K. H. Schweikaert, G. Osswald, and F. Noack, J. Magn. Res. **77**, 825 (1988).
[15] E. Anoardo, E. Romero, D. Pusiol, W. Zaninatti, and C. Marqués, Rev. Fís. Aplicada Instrument. **10**, 55 (1996).
[16] W. H. de Jeu and W. A. P. Claassen, J. Chem. Phys. **68**, 102 (1978).
[17] R. Dong and J. Sandeman, J. Chem. Phys. **78**, 4649 (1983).
[18] N. Vaz, M. Vaz, and W. Doane, Phys. Rev. A **30**, 1008 (1984).
[19] R. Wise, D. H. Smith, and J. W. Doane, Phys. Rev. A **7**, 1366 (1973).
[20] M. A. Osipov, T. J. Sluckin, and E. M. Terentjev, Liq. Cryst. **19**, 197 (1995).
[21] S. T. Lagerwall, B. Otterholm, and K. Skarp, Mol. Cryst. Liq. Cryst. **152**, 503 (1987).
[22] H. Gotzig, S. Grunenberg-Hassanein, and F. Noack, Z. Naturforsch. **49a**, 1179 (1994).
[23] J. Seliger, R. Osredkar, M. Mali, and R. Blinc, J. Chem. Phys. **65**, 2887 (1976).
[24] D. Allender and W. Doane, Phys. Rev. A **17**, 1177 (1978).
[25] R. Blinc, Phys. Rep. **79**, 331 (1981).
[26] A. Wolfenson, D. Pusiol, and A. Brunetti, Z. Naturforsch. **45a**, 334 (1990).
[27] A. E. Wolfenson, A. H. Brunetti, D. J. Pusiol, and W. M. Pontuschka, Phys. Rev. B **41**, 6257 (1990).
[28] S. R. Rabbani, N. Caticha, J. G. dos Santos, and D. J. Pusiol, Phys. Rev. B **51**, 8848 (1995).
[29] R. Kimmich, F. Winter, W. Nusser, and K. H. Spohn, J. Magn. Res. **68**, 263 (1986).
[30] Th. Mugele, V. Graf, W. Wölfel, and F. Noack, Z. Naturforsch. **35a**, 924 (1980).